High efficiency room temperature laser emission in heavily doped Yb:YLF

Matteo Vannini[*1], Guido Toci [1], Daniele Alderighi [1], Daniela Parisi[2], Francesco Cornacchia[2], Mauro Tonelli [2]

[1]*Istituto di Fisica Applicata "Nello Carrara", Consiglio Nazionale delle Ricerche IFAC – CNR Via Madonna del Piano 10, 50019 Sesto Fiorentino (FI), Italy*
[2] *NEST - Dipartimento di Fisica - Università di Pisa, Largo B. Pontecorvo 3 I-56127 Pisa, Italy*
**Corresponding author: M.Vannini@ifac.cnr.it*

Abstract: We report the tunable, CW and quasi CW laser operation at room temperature of an highly doped (30% at.) Yb:YLF crystal longitudinally pumped by a fiber coupled laser diode array. The CW output power is 1.15 W vs. an absorbed pump power of 6 W, with a slope efficiency of 31%. In quasi-CW operation (20% duty factor @10 Hz) an output power of 4 W with an absorbed power of 9.5 W, and a slope efficiency of 62.8% were obtained. The tuning range spans from 1022 to 1075 nm. To our knowledge, these are among the best experimental results obtained at room temperature with Yb doped YLF.

OCIS codes: (140.0140) Lasers and laser optics; (140.3580) Lasers, solid-state; (140.5680) Rare earth and transition metal solid-state lasers; (140.3600) Lasers, tunable; (160.3380) Laser materials.

References and links

1. P. Lacovara, H. K. Choi, C. A. Wang, R. L. Aggarwal, and T. Y. Fan, "Room-temperature diode-pumped Yb:YAG laser," Opt. Lett. **16**, 1089-1091 (1991).
2. T. Y. Fan, "Heat generation in Nd:YAG and Yb:YAG," IEEE J. Quantum Electron. **QE 29,** 1457-1459 (1993).
3. U. Brauch, A. Giesen, M. Karszewski, Chr. Stewen, and A. Voss, "Multiwatt diode-pumped Yb:YAG thin disk laser continuously tunable between 1018 and 1053 nm," Opt. Lett. **20**, 713-715 (1995).
4. A. Lucca, M. Jacquemet, F. Druon, F. Balembois, P. George, P. Camy, J. L. Doualan, and R. Moncorgé, "High-power tunable diode-pumped Yb^{3+}:CaF_2 laser," Opt. Lett. **29**, 1879-1881 (2004).
5. V. Petit, J. L. Doualan, P. Camy, V. Ménard, R. Moncorgè, "CW and tunable laser operation of Yb^{3+} doped CaF_2," Appl. Phys B. **78**, 681-684 (2004).
6. G. Galzerano, P. Laporta, E. Sani, L. Bonelli, A. Toncelli, M. Tonelli, A. Pesatori and C. Svelto, "Room-temperature diode-pumped Yb:KYF_4 laser," Opt. Lett. **31**, 3291-3293 (2006).
7. T. J. Carrig, J. W. Hobbs, C. J. Urbina, A. K. Hankla, G. J. Wagner, C. P. Hale, S. W. Henderson, R. A. Swirbalus, C. A. Denmann, "Single-frequency, diode-pumped Yb:YAG and Yb:YLF lasers," in *Advanced Solid State Lasers*, H. Injeyan, U. Keller, and C. Marshall, eds., Vol. 34 of OSA Trends in Optics and Photonics Series ~Optical Society of America, Washington, D.C., 2000, pp. 144–149.
8. J. Kawanaka, H. Nishioka, N. Inoue, and K. Ueda, "Tunable continuous-wave Yb:YLF laser operation with a diode-pumped chirped-pulse amplification system," Appl. Opt. **40**, 3542-3546 (2001).
9. J. Kawanaka, K. Yamakawa, H. Nishioka, and K. Ueda, "Improved high-field laser characteristics of diode-pumped Yb:$LiYF_4$ crystal at low temperature," Opt. Express **10**, 455-460 (2002).
10. J. Kawanaka, K. Yamakawa, H. Nishioka, and K. Ueda, "30-mJ, diode-pumped, chirped-pulse Yb:YLF regenerative amplifier," Opt. Lett. **28,** 2121-2123 (2003).
11. A. Bensalah, Y. Guyot, M. Ito, A. Brenier, H. Sato, T. Fukuda, and G. Boulon "Growth of Yb^{3+}-doped $YLiF_4$ laser crystal by the Czochralski method. Attempt of Yb^{3+} energy level assignment and estimation of the laser potentiality," Opt. Mater. **26**, 375-383 (2004).
12. L. D. DeLoach, S. A. Payne, L. L. Chase, L. K. Smith, W. L. Kway, and W. F. Krupke "Evaluation of absorption and emission properties of Yb^{3+} doped crystals for laser applications," IEEE J. Quantum Electron. **29**, 1179 (1993).
13. S. Chénais, F. Druon, S. Forget, F. Balembois, and P. Georges, "On thermal effects in solid state laser: the case of Ytterbium-doped materials," Prog. Quantum Electron. **30,** 89-153 (2006).
14. A. Bensalah, Y. Guyot, A. Brenier, H. Sato, T. Fukuda, and G. Boulon "Spectroscopic properties of Yb^{3+}:$LiLuF_4$ crystal grown by the Czochralski method for laser applications and evaluation of quenching processes: a comparison with Yb^{3+}:$YLiF_4$," J. Alloy Compd. **380**, 15-26 (2004).

#81026 - $15.00 USD Received 13 Mar 2007; revised 13 Apr 2007; accepted 14 Apr 2007; published 12 Jun 2007

15. B. F. Aull, H.P. Jenssen "Vibronic interaction Nd:YAG resulting in non reciprocity of absorption and stimulated emission cross section," IEEE J. Quantum Electron. **18**, 925 –930 (1982).
16. P. H. Haumesser, R. Gaume´, B. Viana, and D. Vivien, "Determination of laser parameters of ytterbium doped oxide crystalline materials," J. Opt. Soc. Am. B **19**, 2365-2375 (2002).
17. V. Petit, J. L. Doualan, P. Camy, V. Ménard, R. Moncorgé, "CW and tunable laser operation of Yb^{3+} doped CaF_2," Appl. Phys. B. **78**, 681-684 (2004)

1. Introduction

Ytterbium activated solid state laser are receiving increasing attention in these last years because their interesting and promising characteristics. Yb^{3+} presents only two possible energy levels involved either in the absorption or in the emission: the upper level $^2F_{5/2}$ and the lower $^2F_{7/2}$. This electronic structure allows the obtainment of very efficient laser sources, due to the very low quantum defect (around 10%) high quantum efficiency and absence of excited state absorption, which also result in a small thermal load for the crystal [1-3]. Furthermore, the Stark splitting of the levels involved in the emission and absorption processes determines a wide tunability and it is attracting for the generation or amplification of ultra-fast pulses.

Several hosts, both oxides and fluorides, have been proposed for Yb doping. Although the oxide crystalline materials exhibit superior thermomechanical properties, the fluoride have interesting properties in terms of wider tunability range and longer upper level lifetimes, in comparison to the oxides. Recently, efficient laser operation, wide tunability and possibly large energy storage capabilities have been demonstrated for several Yb doped fluorides, such as CaF_2 [4,5], KYF_4 [6]. Diode pumped CW laser action of a Yb:YLF crystal has been first reported in literature by Carrig *et al*. [7], with a maximum output power of about 230 mW, a slope efficiency of about 17% and a tuning range from 1017 to 1052 nm, using a crystal with 15% wt. doping. Kawanaka *et al*. [8] have proposed this crystal for ultrafast chirped pulse amplification, and they also report diode pumped, CW laser operation in the wavelength range 1027-1053 nm, and a maximum output power in free running operation of 45 mW with 350 mW of absorbed pump power, from a highly doped crystal (40.5% at.). They have also found that cooling the crystal to low temperatures is an effective way to control the population distribution in the lower laser level, reducing the ground level absorption [9]. With this approach, a regenerative amplifier was built using a Yb:YLF operating at the liquid nitrogen temperature [10], with a single pulse energy of 30 mJ and an energy extraction efficiency of 68%. A thorough investigation of the Yb:YLF spectroscopic properties is reported by Bensalah *et al*. [11].

In this paper we report the efficient CW and quasi-CW operation of a diode pumped Yb:YLF laser operating at room temperature. In CW conditions, we obtained an output power of 1.16 W, with a slope efficiency of 31% with respect to the absorbed pump power. The tuning range of the CW laser extended smoothly from 1020 to 1075 nm. We also characterized the behavior of the laser in quasi CW pumping conditions, with a quasi CW output power up to 4 W and a slope efficiency as high as 62.8% when pumping with 20 ms rectangular pump pulses at 10 Hz (i.e. 20% duty factor). To our knowledge, these levels of CW and quasi-CW output power, and quasi-CW slope efficiency are the highest ever reported for a Yb:YLF laser, and they compare well with the performance of other Yb doped fluorides (i.e. CaF_2, KYF). The wavelength span is also wider than the previous results reported for Yb:YLF, and among the wider tuning ranges reported for fluoride crystals.

2. Crystal growth

The crystal we used is a $LiYF_4$ (YLF) single-crystal Ytterbium trivalent doped ion with a concentration of 30 at.% (i.e. 3 out of 10 Y^{3+} ions are replaced by Yb^{3+}). The YLF has tetragonal structure and symmetry group I41/a. The unit-cell parameters are a = 5.2 Å and c = 10.7 Å and the unit cell contains four molecules. The rare-earth dopant substitutionally enters the Y^{3+} sites in S_4 coordination.

The crystal growth apparatus consists of a home-made Czochralski furnace with conventional resistive heating. Special care has been devoted to the quality of the vacuum

#81026 - $15.00 USD Received 13 Mar 2007; revised 13 Apr 2007; accepted 14 Apr 2007; published 12 Jun 2007

system, which has an ultimate pressure limit below 10^{-7} mbar. The sample was grown using LiF and YF_3 powders (from AC Materials, Tampa, Fla, USA) as raw material for the host and a proper amount of YbF_3 powder has been added to achieving the 30% doping in the melt. The resulting weight fractions were 14.4% of LiF, 51.1% of YF_3 and 34.5% of YbF_3. To prevent OH^- contamination, the powders were purified (5N) at AC Materials and the growth process was carried out in a high-purity (99.999%) Argon–CF_4 atmosphere for avoiding contamination of the crystal and to prevent reduction of the Yb^{3+} ions to Yb^{2+} ions. Since the segregation coefficient of Yb in YLF is very close to 1 (see Ref. [11]), here we assume that the concentration in the crystal is the same that in the melt.

The furnace is also equipped with an optical computer-controlled apparatus for diameter control. During growth, the rotation rate of the sample was 5rpm, the pulling rate 0.5 mm/h, and the temperature of the melt was ≈ 860°C. The average size of the YLF crystals was about 12 mm in diameter and 60 mm in length. In Fig. 1 we show the grown boule of Yb:YLF.

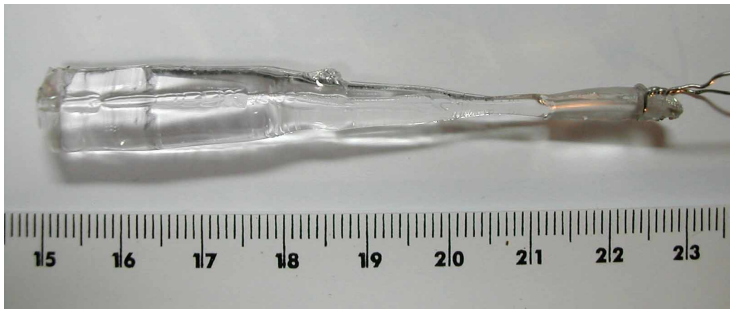

Fig. 1. Boule of YLF: 30% Yb as grown

The single crystalline character of the sample was checked using a X-ray Laue technique that allows us to identify the *c*-crystallographic axis and cut oriented samples.

3. Spectroscopic properties

We performed room temperature absorption measurements by means of a CARY 500 spectrophotometer between 850 and 1080 nm with a resolution of 0.6 nm in the NIR wavelength region; the sensitivity of the instrument is better than $4\cdot10^{-5}$ in absorbance in the NIR region. Furthermore as a first test of the high purity and quality of the crystals we checked that the UV absorption spectrum showed no evidence of incorporation of optically active impurities, this within the sensitivity of the spectrophotometer. In Fig. 2, we report the results obtained for the σ and π polarization for the $^2F_{7/2} \rightarrow {}^2F_{5/2}$ transition. In particular the maximum absorption coefficient is 50 cm^{-1} in π polarization at 958.4 nm, with a full width at half maximum (FWHM) of 9 nm; this value corresponds to a peak absorption cross section $\sigma_{abs}=1.16\cdot10^{-20}$ cm^2, a value that is in agreement with refs. [8, 9], but larger than those reported in refs. [11, 12].

We performed the room temperature fluorescence spectra of the $^2F_{5/2} \rightarrow {}^2F_{7/2}$ transition with the aim to measure the emission cross-section. As a pumping source we used a fiber coupled laser diode tuned at 977 nm. The fluorescence signal was detected perpendicularly to the pump laser direction to avoid pump spurious scattering. The luminescence was chopped and focused by a 75 mm focal length Infrasil lens on the input slit of a 25cm focal length *Jobin-Yvon* monochromator equipped with a 600gr/mm grating (blazed @ 1μm). The resolution of the measurement was 0.6 nm. To record the spectra as a function of the orientation of the samples we used a Glan-Thomson polarizer in front of the input slit of the monochromator. The fluorescence was detected by a liquid nitrogen cooled InSb detector, fed into pre-amplifiers, processed by a lock-in amplifier linked to the and acquired on a PC. The

#81026 - $15.00 USD Received 13 Mar 2007; revised 13 Apr 2007; accepted 14 Apr 2007; published 12 Jun 2007

spectra were normalized for the optical response of the system using a black-body source at 3000 K.

We measured the room temperature fluorescence decay-time for the $^2F_{5/2}$ manifold. The crystals were excited by a pulsed tunable Ti:Al_2O_3 laser (pumped by a doubled Nd:YAG pulsed laser) with 10 Hz repetition rate, 30 ns pulse width tuned at 930nm. Furthermore the power incident on the sample was reduced by means of attenuators to suppress reabsorption artifacts and non-linear effects as much as possible; we estimated the incident energy less than 0.5 μJ. We collected the signal from a short portion of the sample (≈ 1 mm) to have the energy density as constant as possible in the observed region. The dynamic fluorescence was detected by the same experimental apparatus described above, but the signal was detected by an S1 cathode photomultiplier and sent, by fast amplifiers, to a digital oscilloscope connected to a computer.

The decay time curve exhibits a single exponential behavior that has been fit with a value of τ=3.0 ± 0.3 ms. In Ref. [12, 13], the authors reported 2.2 ms for low concentrated Yb:YLF samples. The disagreement can be easily explained considering that all highly doped Yb crystals undergo to radiation trapping effect despite the attention in the measurements; because of this phenomenon the measured decay time becomes longer as the dopant concentration is increased. For example in Ref. [14] the authors report 3.18 ms for a 10% Yb:YLF sample: as explained in the same reference this difference can be due to the self quenching mechanism that becomes important for Yb concentrations larger than 10-15%.

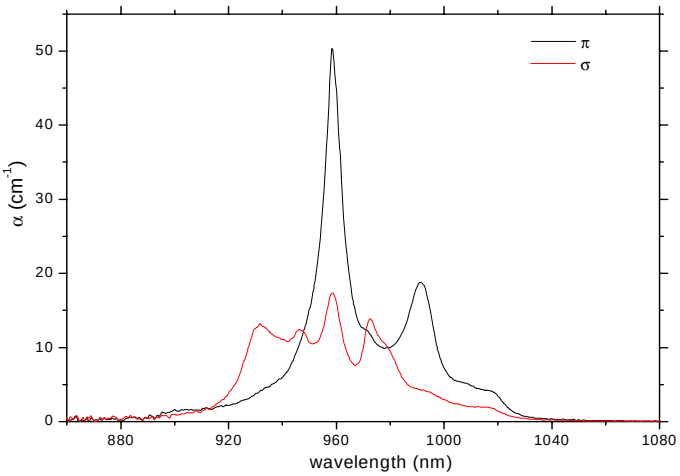

Fig. 2. Room temperature absorption spectra for the YLF: 30% Yb

Using the lifetime value found in the literature, we evaluated the emission cross sections by the β–τ method (Ref. [15]). Since we have experienced reabsorption effects in the decay time measurements, the calculated emission cross sections have been compared in Figs. 3(a), 3(b) with the emission cross sections obtained by the reciprocity method. This method allows to calculate the emission cross sections once the absorption and the energy level positions are known:

$$\sigma_{em} = \frac{\alpha}{N} \cdot \frac{Z_l}{Z_u} \cdot \exp\left[\frac{E_{ZL} - h\upsilon}{kT}\right] \tag{1}$$

where α is the absorption coefficient (in cm^{-1}), N indicates the dopant ion density, Z_i are the partition functions of the upper (u) and lower (l) manifold, E_{ZL} represents the zero-phonon line position (in cm^{-1}). The energy level data are from Ref. [11]. The analysis of Fig. 3 shows how

#81026 - $15.00 USD Received 13 Mar 2007; revised 13 Apr 2007; accepted 14 Apr 2007; published 12 Jun 2007

the cross sections calculated from the emission spectra are underestimated in the short wavelength region because of the strong reabsorption, leading to incorrect evaluation of the peak values. On the other side the reciprocity method is not suitable to reproduce the correct trend in the longer wavelength region [16]. Nevertheless the agreement in the intermediate region (peaks around 1020 nm) is satisfactory. The peak value is $10.9 \cdot 10^{-21} cm^2$ (considering the reciprocity method) at the wavelength of 992.6 nm in π polarization; the most interesting peak for laser application is the one around 1018 nm in both σ and π polarization, $3.4 \cdot 10^{-21}$ cm^2 and $8.3 \cdot 10^{-21}$ cm^2 respectively. The reported values are in agreement with Ref. [12].

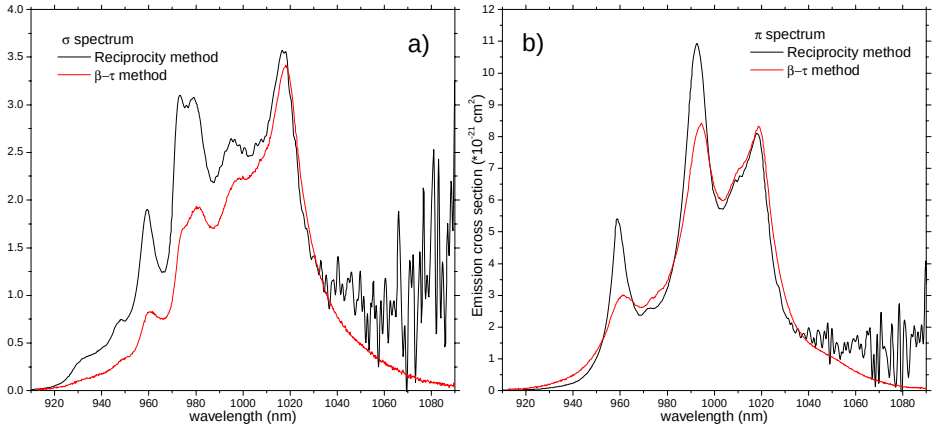

Fig. 3. Room temperature polarized emission cross section for the YLF 30% Yb

4. Experiment

The crystal we employed in the measurements had a thickness of 1.5 mm, and a cross section of 4x5 mm^2, polished for laser quality. The optical axis c was parallel to the crystal facets. As a pump we used a diode laser array mod. HLU25F200-940, by LIMO GmbH coupled with a 200 μm output fiber. The pump laser maximum emission power was 25 W, at a wavelength of about 940 nm, with a bandwidth of about 4 nm FWHM. The diode emission wavelength has a slight dependence from the diode heat sink temperature (about 0.35 nm/°C around room temperature) and from the pump current (around 0.16 nm/A)

In Fig. 4 we report the experimental set-up for the laser cavities used in the experiment. The inset shows the layout for a tunable laser cavity.

The pump beam coming out from the fiber is unpolarized and has a Numerical Aperture (NA) of 0.4. The pump beam is recollimated and then refocused by a pair of achromatic doublets (Melles Griot model LAO079, focal lenght 60 mm) through the cavity end mirror EM and then into the crystal, with a magnification of about 1:1. The pump beam spot at the Yb:YLF crystal surface has an almost gaussian profile with a radius @ $1/e^2$ of 155 μm.

The end mirror EM is flat, with a dichroic coating (by CVI Corp.) having high transmission @ 940nm and high reflectivity for wavelengths greater than 1020 nm. The overall transmission of the pump chain (from the fiber tip to the crystal surface) is 78 % at the diode laser emission wavelength.

The crystal is placed at about 3 mm from the end mirror EM, in the focus of the pump beam (Fig. 4). It absorbs about 58% of the incident pump beam power at low power level (i.e. as low as 0.57 W). The absorption slightly saturates down to a value of about 55% for an incident power of 15.5 W. The crystal is longitudinally cooled from the side facing the mirror FM by means of a copper heat sink held at a temperature of 18°C by a Peltier cooler. Indium

#81026 - $15.00 USD Received 13 Mar 2007; revised 13 Apr 2007; accepted 14 Apr 2007; published 12 Jun 2007

foil gaskets were used to improve the thermal contact between the crystal and the heat sink. The crystal is aligned with the facets perpendicular to the cavity axis, and a particular care was put to re-aligning the Fresnel reflections from the crystal facets backward on the incoming beam, to minimize the losses. The laser cavity is V-shaped, with a folding half angle of 10°. The folding mirror FM has a curvature radius of 150 mm. OC is the flat output mirror. The lengths of the two cavity arms, L1 and L2, were set to 77mm and 470mm respectively, resulting in a stable confocal cavity with a mode radius w_0 of about 50 μm at the waist at EM. Average power measurements were carried out by means of thermopile detectors (OPHIR NOVA with a thermopile head mod. 2A SH or OPHIR DGX with a thermopile head 30A-P-CAL for higher mean power). The residual pump transmitted by the crystal was suppressed by means of a long-pass filter LP1000 (average transmission 75% in the laser bandwidth, high reflectivity to the pump, cut-off wavelength at about 1000nm) placed in front of the power meter.

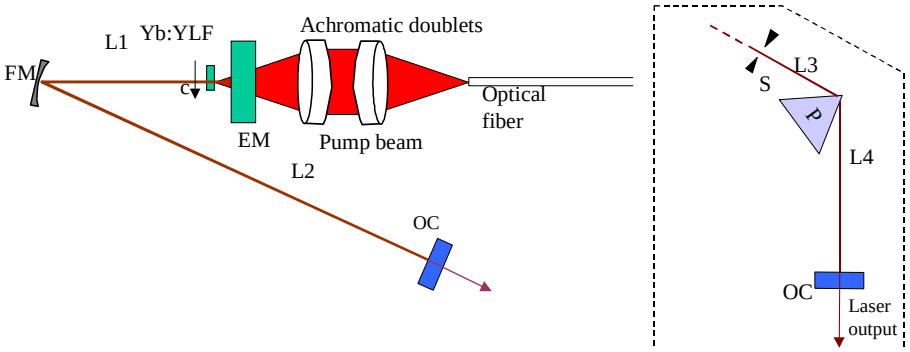

Fig. 4. Layout of the laser cavity. EM: End mirror, flat, FM: folding mirror (radius of curvature 150 mm); OC: output coupler, flat ; the arrow marked with c denotes the direction of the crystal optical axis. The inset shows the configuration of the cavity arm between FM and OC as used for the tunable laser, where P: tuning prism; S: slit.

5. Output power measurements and slope efficiency determination

With the experimental set up described above, we characterized the CW laser behavior of the system. In Fig. 5 we report the laser output power as a function of absorbed pump power, obtained with an output coupler with transmission 6% at 1050 nm. The lasing threshold is at an absorbed power of about 1.9 W, corresponding to a peak absorbed intensity of 5.0 kW/cm^2. This value is about an order of magnitude lower than that reported by Kawanaka *et al* [8] (i.e. 45 kW/cm^2 of absorbed intensity), despite the lower transmission of the output coupler (i.e. 1.5% at the lasing wavelength) used in that case. Such a higher threshold level, even in presence of lower output coupling losses, could be due to higher scattering losses in the crystal, or possibly a poor matching between the pump beam and the cavity mode.

The dependence of the output power from the absorbed power is slightly superlinear. This is due to the saturation of the absorption from the lower level of the laser transition at the lasing wavelength. This absorption is due to the thermal population of the laser lower level (because of the quasi-three level structure). The saturation of this absorption for increasing intracavity power reduces the overall round trip percentual losses, thus increasing the overall laser efficiency. The slope efficiency for a pump power ≥4 W is 31%. The lasing wavelength peak is around 1049 nm, with a FWHM of about 2 nm, but we observed a slight increase in the emission wavelength for increasing pump power, from 1048.6 to 1050 nm. The output beam had a smooth gaussian profile, with an M^2 factor of 3.5, as determined by acquiring the beam intensity distribution cross sections in the focus of a suitable lens, by means of a CCD camera and a beam analyzer software. This rather high value is probably due to the mismatch between the radii of the pump beam and of the cavity TEM_{00} mode. The laser beam is

#81026 - $15.00 USD Received 13 Mar 2007; revised 13 Apr 2007; accepted 14 Apr 2007; published 12 Jun 2007

polarized in the plane of the *c* axis of the crystal (i.e. in the plane of Fig. 4), with a polarization ratio higher than 100:1.

To assess the influence of the thermal load imposed by the pump beam on the crystal, we characterized the laser performances of the crystal in quasi-CW (QCW) pumping conditions. The diode laser was modulated to obtain rectangular pump pulses, at a repetition frequency of 10 Hz, with increasing duty factors from 40% up to 100%, with a rise and fall time of around 50 μsec (i.e. almost negligible with respect to the pulses duration). The laser output pulses had a rectangular shape, with the same pulse duration of the pump. During each pump pulse the laser action develops in CW mode, but the crystal undergoes an average thermal load that is only a fraction (equal to the duty factor) of the thermal load that would result in true CW conditions. The results of this characterization are shown in Fig. 5(a). At a given pump power, for decreasing duty factor the output power increases, as well as the slope efficiency, whereas the threshold power is substantially unaffected. In particular the slope efficiency reaches a value as high as 42 % (with respect to the absorbed pump power) at a duty factor of 40%.

This behavior is probably due to the fact that at lower duty factors, the reduction of the crystal temperature in the pumped region determines a corresponding decrease of the absorption from the lower laser level at the lasing wavelength, due to the reduction of the thermal population in this level.

In order to characterize the performance of the laser in quasi-CW operation, we pumped the laser with a low duty factor (20%), up to an instantaneous absorbed power level of 9.5 W. The results are reported in Fig. 5(b). In this condition it was possible to use a instantaneous power level higher than that used with higher duty factors, due to the reduced average thermal load on the crystal. The slightly superlinear behavior of the output power with respect to the input power, that was already observed in the measurements at higher duty factors, is even more evident here because of the wider span in the absorbed power. The slope efficiency, calculated for an absorbed power in the interval 4 – 6 W [i.e. in the same interval used for the slope efficiencies reported in Fig. 5(a)] is 54.3%. In the final part of the curve, for instantaneous absorbed power between 6 W and 9.5 W, the resulting slope efficiency (η) is as high as 62.8%. The overall power conversion efficiency (i.e. the ratio of the output power with respect to the absorbed power) is 42% at the maximum absorbed power level. The resonator did not need any realignment among all the measurements shown in Fig. 5 (b).

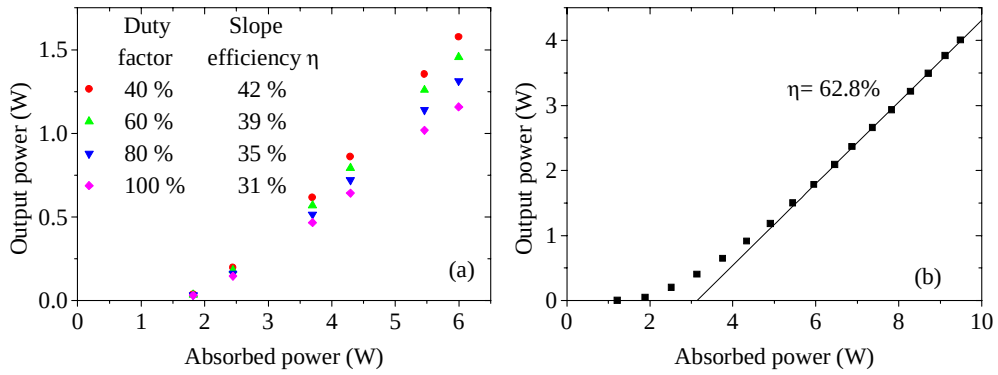

Fig. 5. Instantaneous output power vs. instantaneous absorbed power, for different pump duty factors (from 40% to 100% in (a), 20% in (b)). The OC transmission is 6%, the free running lasing wavelength is around 1049 nm. The slope efficiencies reported in the graphs are calculated for an absorbed power higher than 4 W in (a), 6 W in (b).

#81026 - $15.00 USD Received 13 Mar 2007; revised 13 Apr 2007; accepted 14 Apr 2007; published 12 Jun 2007

6. Output tuning test

We built a tunable laser cavity based on the design described before, by adding a tuning prism in the cavity arm between the tuning mirror and the output coupler, as exemplified in the inset of Fig. 4. The prism was made of SF10 glass, with an apex angle of 60°, corresponding about to the Brewster input and output angle when the prism is set in the minimum deviation configuration. To increase the wavelength selectivity of the cavity, a slit was placed between the folding mirror FM and the prism. The distance between the mirror FM and the prism apex L3 was set to 315 mm, and that from the prism apex to the mirror OC L4 was set to 125 mm. The laser output was tuned by tilting the mirror OC around an axis perpendicular to the prism dispersion plane. The wavelength measurements were performed by means of a 60 cm focal length spectrometer equipped with a multichannel spectrum analyzer, with an overall resolution of 0.4 nm.

The tuning curves obtained with an OC having a transmission of 2% in the range 1020 – 1080 nm, at various CW pumping levels, are shown in Fig. 6. It can be seen that the laser tunes smoothly from about 1030 to 1074 nm. A low power tail in the tuning curve reaches a wavelength as short as 1022 nm. On the side of the shorter wavelengths, the tuning range is somewhat limited by the drop in the reflectivity of the end mirror EM, which has a transmission of 1% at 1020 nm, and a transmission as high as 10% at 1000 nm. The output spectrum for a given tuning position was rather broad and structured, with several secondary peaks and with an average width (evaluated as the square root of its second moment about the mean) of about 2.5 nm. This spectral width was obtained with a slit width of about 2 mm, and it can be reduced by narrowing the aperture of the slit, but at the price of a reduction in the output power and in a narrowing of the tuning range, due to the higher diffraction losses produced by the slit.

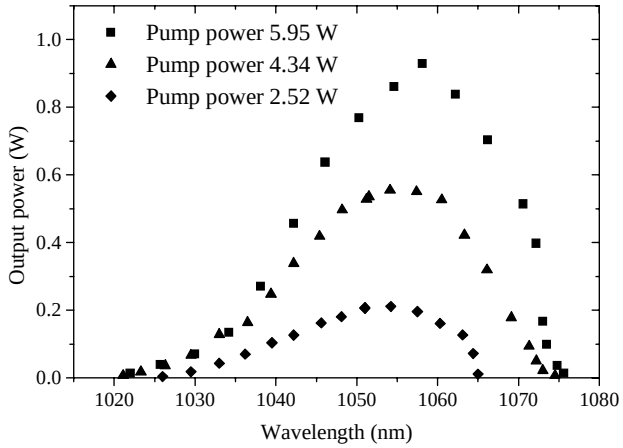

Fig. 6. CW output power as a function of wavelength for various absorbed pump power levels. The transmission of the output coupler is 2%

7. Conclusions

In this work we have reported infrared tunable laser emission achieved by means of a YLF single crystal heavily doped (30% at.) with Yb^{3+} ions. In this respect our experimental results at room temperature are a net improvement, in terms of output power and slope efficiency with respect to the lasing action reported in previous experiments dealing both with mildly doped [7] and heavily doped crystals [8]. Our results show that this crystal can be an interesting laser medium, even at room temperature. In particular the long lifetime of the

#81026 - $15.00 USD Received 13 Mar 2007; revised 13 Apr 2007; accepted 14 Apr 2007; published 12 Jun 2007

upper laser level τ= 2.2 ms (as reported in Refs. [12, 13]) is among the longest available from other Yb doped crystals, both oxides and fluorides. This makes Yb activated YLF very suitable for energy storing systems, such as high energy, low repetition rate pulsed oscillators, regenerative amplifier, chirped pulsed amplification (CPA) systems, etc. Using the lifetime value reported in the literature for low concentrated samples we calculated the emission cross section which resulted in good agreement with ref. [12] especially where the reabsorption was quite negligible (longer wavelength). A slope efficiency as high as 62.8% was achieved pumping with a duty factor of 20% @10Hz, with an instantaneous output power of 4 W. Conversely, pumping in CW we obtained an output power of 1.15 W with a slope efficiency of 31%. Introducing an intracavity prism we were able to tune our laser in the range of 1022-1074 nm. Other authors reported comparable values when using other Yb doped fluorides. For instance, with Yb:CaF_2 a slope efficiency of 50.1% with respect to the absorbed power, and a tuning range from 1000 to 1060 nm were obtained under CW pumping at 920 nm [17]; with Yb:KYF_4 Galzerano *et al*. [6] have reported a slope efficiency of 43%, (with respect to the incident pump power) and a tuning range from 1010 to 1080 nm under CW pumping at 980 nm. Regarding the Yb:YLF, Kawanaka *et al.* [8] have reported a slope efficiency of 50% when operating at room temperature, but with a maximum output power of only 45 mW; when operating at cryogenic temperatures [9] they obtained a maximum power of 110 mW, with a slope efficiency of 25 %.

Our results show therefore that the performances of the Yb:YLF crystal operating at room temperature are comparable with those of other Yb doped fluorides, and that this crystal does not need to operate at cryogenic temperature in order to achieve good laser performances.

#81026 - $15.00 USD Received 13 Mar 2007; revised 13 Apr 2007; accepted 14 Apr 2007; published 12 Jun 2007